



Fermi National Accelerator Laboratory

FERMILAB-Conf-98/228-E

CDF

The Measurement of the Mass of the W Boson from the Tevatron

R. Thurman-Keup
For the CDF Collaboration

*Fermi National Accelerator Laboratory
P.O. Box 500, Batavia, Illinois 60510*

August 1998

Published Proceedings of the *2nd Latin America Symposium on High-Energy Physics (SILAFAE 98)*,
San Juan, Puerto Rico, April 8-11, 1998

Disclaimer

This report was prepared as an account of work sponsored by an agency of the United States Government. Neither the United States Government nor any agency thereof, nor any of their employees, makes any warranty, expressed or implied, or assumes any legal liability or responsibility for the accuracy, completeness, or usefulness of any information, apparatus, product, or process disclosed, or represents that its use would not infringe privately owned rights. Reference herein to any specific commercial product, process, or service by trade name, trademark, manufacturer, or otherwise, does not necessarily constitute or imply its endorsement, recommendation, or favoring by the United States Government or any agency thereof. The views and opinions of authors expressed herein do not necessarily state or reflect those of the United States Government or any agency thereof.

Distribution

Approved for public release; further dissemination unlimited.

CDF/PUB/ELECTROWEAK/PUBLIC/4676
Version 1.0
July 21, 1998

The Measurement of the Mass of the W Boson from the Tevatron

Randy Thurman-Keup

*Argonne National Lab
9700 South Cass Avenue
Argonne, IL 60439*

*Presented at the Second Latin American Symposium on High Energy
Physics, April 8-11, 1998, in San Juan, Puerto Rico.*

The Measurement of the Mass of the W Boson from the Tevatron

Randy Thurman-Keup¹

*Argonne National Lab / HEP-362
9700 South Cass Avenue
Argonne, IL 60439*

Abstract. This paper presents measurements of the mass of the W vector boson from the CDF and $D\bar{O}$ experiments using data collected at $\sqrt{s} = 1.8$ TeV during the 1994-1995 data taking run. CDF finds a preliminary mass of $M_W = 80.43 \pm 0.16$ GeV and $D\bar{O}$ measures a mass of $M_W = 80.44 \pm 0.12$ GeV.

I INTRODUCTION

During the 1994-1995 collider run of the Fermilab Tevatron, the CDF and $D\bar{O}$ experiments collected data corresponding to integrated luminosities of 90 pb^{-1} and 82 pb^{-1} respectively. From this data, CDF extracted $\sim 21,000$ $W \rightarrow \mu\nu$ events while $D\bar{O}$ obtained $\sim 28,000$ $W \rightarrow e\nu$ events. These W events were used to make measurements² of the mass of the W boson [1].

A Motivation

When going from tree level in the Standard Model (SM) to next-to-leading order, the relation between the mass of the W boson and the other SM parameters gets modified as follows:

$$M_W^2 = \left(\frac{\pi\alpha_{EM}(0)}{\sqrt{2}G_F \sin^2 \theta_W} \right) \longrightarrow \left(\frac{\pi\alpha_{EM}(M_Z^2)}{\sqrt{2}G_F \sin^2 \theta_W} \right) \frac{1}{1 - \Delta r}, \quad (1)$$

where Δr embodies the loop corrections to the W propagator [2]. The dominant contributions to the corrections come from the top quark which introduces a quadratic dependence on its mass, and the higgs boson which produces a logarithmic dependence on its mass. These dependencies allow one to probe for the higgs given a precision measurement of the W mass. In addition, Standard Model

¹⁾ representing the CDF and $D\bar{O}$ collaborations

²⁾ The CDF measurement is only a preliminary measurement.

extensions and/or replacements produce their own corrections and here again, a precision measurement may be used to uncover these theories.

B Tevatron Environment

The majority of W events at the Tevatron are produced from s channel quark-antiquark interactions. The W 's of interest in this measurement are the ones that decay to muon-neutrino or electron-neutrino pairs, since these are the cleanest decays. Unfortunately, the fact that the neutrino is undetected, prevents us from measuring the invariant mass of the W . One could infer the neutrino 3-momentum by requiring momentum conservation in the event if it weren't for the fact that the energy of the incident quarks is not known. Unlike electron-positron colliders, the quarks are bound inside the (anti)protons and their momentum is governed by parton distribution functions (PDFs). Fortunately we can still enforce momentum conservation in the plane transverse to the beam direction since the incident quarks have essentially no transverse momentum.

This leaves us with two possible quantities from which to extract the mass: the transverse momentum of the lepton, p_T^ℓ , or the transverse mass of the lepton-neutrino pair, $M_T = \sqrt{2p_T^e p_T^\nu (1 - \cos \Delta\phi)}$. The transverse mass is analogous to the invariant mass except that only components of momentum transverse to the beam are used. The transverse mass is less sensitive than p_T^ℓ to the transverse momentum of the W^3 and is upwardly bounded by M_W thereby still providing sensitivity to the mass. It is, however, more sensitive to the energy resolution of the calorimeter (see Sec. III A) since it depends on the inferred momentum of the neutrino. Which method is ultimately chosen depends on the relative precision of the measurement of the transverse momentum distribution of the W (increased systematic uncertainty in p_T) when compared to the calorimeter resolution (increased statistical uncertainty in M_T). In the present case, M_T wins.

C Event Selection

The signature for W events is a high momentum muon or electron ($p_T > 25$ GeV)⁴, and large missing energy from the undetected neutrino ($\cancel{E}_t > 25$ GeV). This missing energy is the transverse momentum needed to balance the visible transverse momentum in the event. The visible momentum is the sum of the muon or electron momentum and a vector sum of the energy in the calorimeter towers of the detector (not including the energy from the lepton of course; see Sec. III A). The lepton must be central ($|\eta| < 1$) and satisfy various quality cuts. For $D\bar{O}$, these cuts require the electron to be isolated, to have a calorimeter shower shape consistent with Monte Carlo expectations, and to have a track pointing at the calorimeter

³⁾ Corrections are of $\mathcal{O}(\beta^2)$ compared with $\mathcal{O}(\beta)$ for p_T^ℓ .

⁴⁾ Throughout this paper, $\hbar = c = 1$; thus mass, momentum, and energy all have units of eV.

cluster. For CDF, the muon is required to have deposited energy in the calorimeter consistent with a minimum ionizing particle, to have a track pointing at the hits in the muon chambers, and to *not* be consistent with a cosmic ray. There is also a requirement that the vector sum of the energy in the calorimeter (not including the contribution from the lepton), \vec{u} , be less than 15 GeV for DØ and less than 20 GeV for CDF. This serves to further reduce the background from QCD inspired processes and results in cleaner events. After these requirements are placed on the data sample, CDF has 21,000 W 's remaining and DØ has 28,000 W 's left.

There are other datasets that are used in this analysis, chief among them being $Z \rightarrow \ell^+ \ell^-$. The requirements on Z events are similar to W 's for one lepton and typically loosened somewhat for the other lepton resulting in 2200 Z 's for DØ and 1400 Z 's for CDF.

II LEPTON MOMENTUM CALIBRATION

CDF and DØ take similar approaches to calibrating the energy scale for the lepton. Both involve comparing measured mass resonances with known mass values. In the case of CDF, $J/\psi \rightarrow \mu\mu$ decays are used to set the momentum scale of the tracking chamber; at DØ, $Z \rightarrow ee$, $\pi^0 \rightarrow \gamma\gamma$, and $J/\psi \rightarrow ee$ are used to set the energy scale of the calorimeter.

A CDF Momentum Scale

The momentum scale of the tracking chamber / magnetic field is set using the invariant mass distribution of $\sim 250,000$ $J/\psi \rightarrow \mu\mu$ events (Fig. 1), which is fit using a simulated lineshape. The data are corrected for magnetic field variations over the course of data taking and the momenta are corrected for energy lost in the material before the tracking chamber. The J/ψ simulation includes QED radiative contributions and both prompt and B decay sources of J/ψ 's. These two effects can be seen in Figure 1. The latter is important because the tracks from the muons are constrained to originate from the beamline which introduces a systematic bias in tracks that did not originate from the beamline. This beam constraint is applied to J/ψ events to uncover any possible unknown biases that may affect the W mass measurement.

Fitting the lineshape to the J/ψ data results in a mass of 3096.2 ± 1.5 MeV. This translates to a momentum scale of 0.99977 ± 0.00048 leading to an uncertainty of 40 MeV on the W mass. The dominant uncertainties in the momentum scale are the dE/dx energy loss correction and the extrapolation of the momentum scale from the J/ψ mass to the W mass.

Muon Energy Loss – The muons from J/ψ decays traverse material before entering the tracking volume and thus lose energy. The amount of energy they lose depends on the amount and type of material. The amount of material can be obtained using photon conversions to electron-positron pairs. These conversions

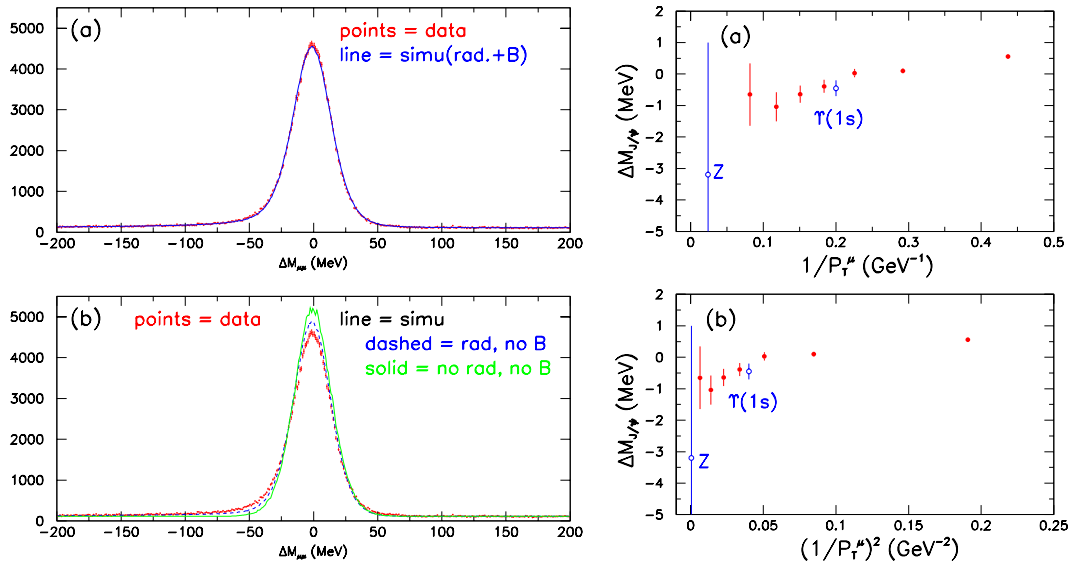


FIGURE 1. Left: a) Invariant mass distribution of $J/\psi \rightarrow \mu\mu$ events. b) The effect of adding various features to the simulation. Right: J/ψ mass as a function of a) inverse p_T^μ and b) inverse $(p_T^\mu)^2$.

are used to map out the material in the inner detector, and when combined with knowledge about the composition of the various structures provide the necessary corrections. The uncertainty of 1.0 MeV produced in the J/ψ mass is due to uncertainties in the material types in the various regions and to residual variation in the J/ψ mass with region.

Extrapolation to the W – The momentum scale is obtained using muons from J/ψ decays which have an average momentum of 4 GeV. This is a long way from the typical 38 GeV momenta of W decay muons. Fortunately the relevant quantity is not momentum but inverse momentum, which is proportional to the curvature of the track. This is what the tracking chamber measures and where deviations from expected behavior should occur. Figure 1 shows the variation of J/ψ mass with inverse momenta. The advantage is that the distance in inverse momenta from the J/ψ to the W is shorter than the spread in the J/ψ data making for an effortless extrapolation. Since the extrapolated difference is small and since wrong dE/dx corrections, for example, can fake a variation here, it is taken as an uncertainty rather than a correction. This uncertainty, if expressed in terms of the J/ψ mass, is also 1.0 MeV.

B DØ Energy Scale

The DØ calorimeter is a Uranium/Liquid Argon sampling calorimeter which, since the LAr has unit gain, is extremely stable over time. This enables electron testbeam data to be used to obtain a simple functional form for the energy scale

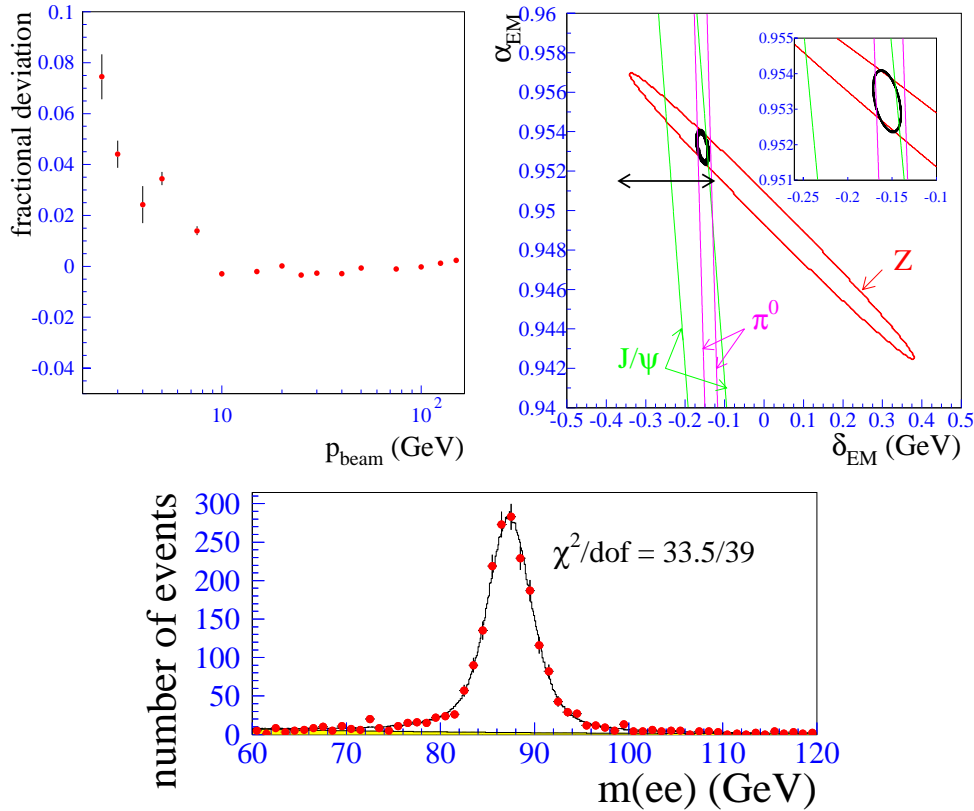


FIGURE 2. Top Left: Deviations from the expected response for the DØ electromagnetic calorimeter for electrons as a function of the electron energy. Top Right: The contours in the scale parameter’s plane for $J/\psi \rightarrow ee$, $\pi^0 \rightarrow \gamma\gamma$, and $Z \rightarrow ee$. The thick contour is all three combined including only the statistical component. The double arrow indicates the systematic uncertainty in δ due to deviations in the testbeam results at low energy (top left plot). Bottom: Invariant mass distribution of electron pairs near the Z compared with simulation where the simulation is adjusted for the energy scale to allow comparison with data.

(Fig. 2). The testbeam results indicate that the calorimeter response is very linear and only deviates from the expected response below 10 GeV. Thus a linear function is used to relate the true energy to the measured energy, $E_{meas} = \alpha_{EM}E_{true} + \delta_{EM}$. The deviations from this linear behavior are treated as systematic uncertainties.

Like CDF, DØ determines the constants in the above equation by comparing mass resonances with known masses. Three resonances are used: $J/\psi \rightarrow ee$, $\pi^0 \rightarrow \gamma\gamma$, and $Z \rightarrow ee$.

$J/\psi \rightarrow ee$ Decays – The relation between the measured J/ψ mass peak and the J/ψ mass is determined from simulation to be $m(ee) = \alpha_{EM}m_{J/\psi} + 0.56\delta_{EM}$. This equation defines a contour in the α_{EM} - δ_{EM} plane (Fig. 2).

$\pi^0 \rightarrow \gamma\gamma$ Decays – The decay $\pi^0 \rightarrow \gamma\gamma$ is detected by identifying the electrons

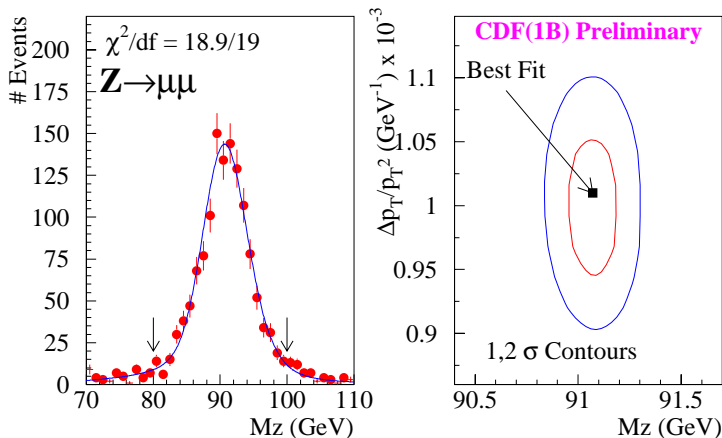


FIGURE 3. Left: Invariant mass distribution of $Z \rightarrow \mu\mu$ events from CDF. The width of the peak is a convolution of the linewidth of the Z and the momentum resolution. Right: Contours in momentum resolution and mass with best fit point.

resulting from the conversions of the two photons⁵. Because the calorimeter clusters from the 4 electrons overlap, a quantity called the symmetric mass is constructed which is equal to the invariant mass if the energy of the two photons is equal. As with the $J/\psi \rightarrow ee$ decays, a similar equation relating the symmetric mass to the actual mass can be obtained and again results in a contour in the $\alpha_{EM}-\delta_{EM}$ plane (Fig. 2).

$Z \rightarrow ee$ Decays – Both the previous resonances are low masses and as such do a good job of constraining δ_{EM} but do a poor job of constraining α_{EM} . To constrain α_{EM} the $Z \rightarrow ee$ resonance is used. The Z has the added benefit that the decay electrons are not monochromatic thus providing another albeit weak measurement of δ_{EM} . Again, a contour in $\alpha_{EM}-\delta_{EM}$ is found and together with the J/ψ and π^0 provides a tight constraint on α_{EM} and δ_{EM} (Fig. 2). The best fit returns $\delta_{EM} = -0.16^{+0.03}_{-0.21}$ GeV and $\alpha_{EM} = 0.9533 \pm 0.0008$ where the uncertainties include systematic contributions.

C Energy and Momentum Resolutions

The lepton energy or momentum resolution is obtained by fitting for the width of either the $Z \rightarrow ee$ ($D\phi$; Fig. 2) or $Z \rightarrow \mu\mu$ (CDF; Fig. 3) distributions.

The electron energy resolution for $D\phi$ is parameterized as

$$\frac{\sigma_E}{E} = \frac{13.5\%}{\sqrt{E \sin \theta}} \oplus \kappa \oplus \frac{n}{E} \quad (2)$$

where the first term (stochastic) is determined from testbeam data and the last term (n/E) is the contribution from other energy in the event and is determined

⁵⁾ Each of the two conversion pairs appears as a doubly ionized track in the tracking chamber

from calorimeter towers near the electron. The constant term, κ , is measured from the width of the Z and is found to be $(1.15_{-0.36}^{+0.27})\%$.

The momentum resolution for CDF is parameterized as $\sigma_{1/p_T} = \kappa \cdot (1/p_T)$ since the tracking chamber measures the curvature of a track which is proportional to $1/p_T$. The constant is extracted from the width of the Z and is $(0.101 \pm 0.005)\%$.

III RECOIL MEASUREMENT AND CALIBRATION

A Recoil Measurement

There are only two quantities to measure in every W event: the lepton p_T , and the transverse recoil momentum, \vec{u} , from the p_T of the W . Together they can be used to infer the neutrino p_T . The recoil momentum is defined as $\vec{u} = \sum_i (E_i \cdot \sin \theta_i) \hat{\phi}_i$ where the sum runs over calorimeter towers and θ and $\hat{\phi}_i$ are the polar angle and azimuthal unit vector of the tower containing energy E . The towers containing energy deposited by the lepton are removed from the sum; however, the removed towers also contain small contributions from the recoil which must be accounted for. The CDF measurement replaces the removed towers with an average recoil event energy determined from nearby towers. The DØ measurement on the other hand duplicates the removal in the simulated data and also corrects the simulated electron energy to account for this small recoil contamination.

B Recoil Calibration

The calibration of the recoil measurement is obtained from Z data where the recoil measurement can be compared to the p_T of the Z measured with the leptons. There is a slight complication in that \vec{u} contains not only the recoil energy but also the energy from the (anti)proton breakup plus any overlapping $\bar{p}p$ interaction. Thus the calibration also includes a minimum bias component.

DØ Calibration — The parameterization of \vec{u} is given by

$$\vec{u} = \left[R_{rec} \vec{q}_T + s_{rec} \sqrt{R_{rec} q_T} \hat{q}_t \right] - \Delta \vec{u} + \alpha_{mb} \vec{E}_T^{mb} \quad (3)$$

$$R_{rec} = \alpha_{rec} + \beta_{rec} \log(q_T) \quad (4)$$

where R_{rec} represents the recoil response, s_{rec} is the response resolution, Δu is the small correction for the tower removals mentioned in Section III A, and the last term is a literal minimum bias event weighted by α_{mb} .

The form of R_{rec} is obtained from a Herwig-Geant $Z \rightarrow ee$ simulation (Fig. 4) and does a good job of describing the DØ jet response. Z data is used to constrain the parameters α_{rec} and β_{rec} and the values obtained ($\alpha_{rec} = 0.693 \pm 0.060$ and $\beta_{rec} = 0.040 \pm 0.021$) agree with the Herwig-Geant values of 0.713 and 0.046. The parameter s_{rec} is the recoil part of the resolution parameterization and is also

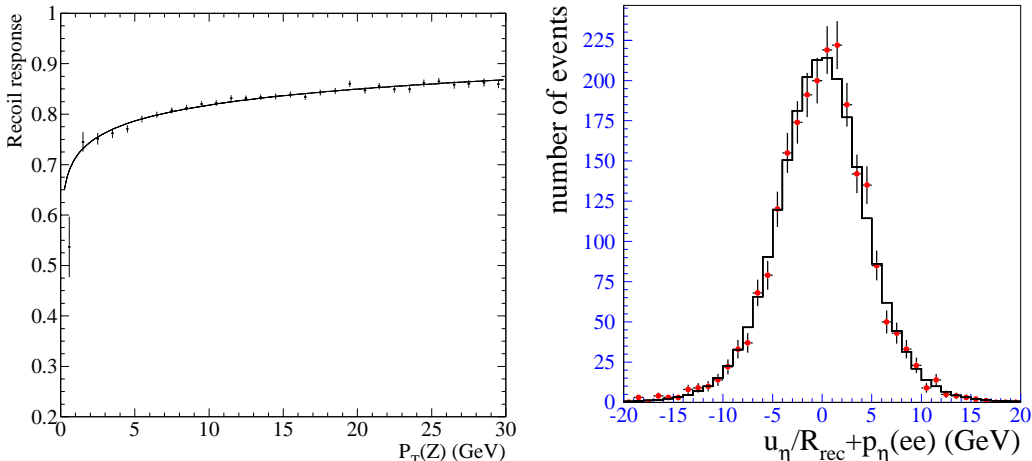


FIGURE 4. Left: Simulated detector response to recoil from Z 's in Herwig-Geant $Z \rightarrow ee$ simulation. Right: Difference between p_η and u_η after being corrected by the response function. The points are the data and the histogram is the simulation. This distribution should have a mean of zero and a width characteristic of the recoil resolution. (η is the angular bisector of the two electrons and is the axis with the least sensitivity to the electron energy resolution.)

obtained from $Z \rightarrow ee$ events along with the parameter α_{mb} representing the non-recoil part of the resolution. This non-recoil part is modeled by a minimum bias event (chosen such that the luminosity distribution is the same as in the Z data) multiplied by a weight, α_{mb} , which is constrained by the Z data⁶. Comparisons of Monte Carlo $Z \rightarrow ee$ events with data in Figure 4 show good agreement in both the mean of the distribution (response) and the width (resolution).

CDF Calibration — The CDF parameterization of \vec{u} is

$$\vec{u} = R_{rec} \vec{q}_T + S \vec{\sigma}_{mb} \quad (5)$$

$$R_{rec} = \alpha_{rec} + \beta_{rec} e^{-\lambda q_T} \quad (6)$$

where, as with $D\phi$, R_{rec} is the recoil response and, unlike $D\phi$, all the resolution is contained in the second term.

The form of R_{rec} is obtained from Z data and is plotted in Figure 5. The parameters are additionally constrained by W data distributions to improve the uncertainty in the recoil response.

The resolution term handles both resolution from the minimum bias contribution and from the recoil response resolution. This works because for most W 's, the recoil tends to look like the minimum bias contribution and thus one resolution is a fairly good approximation. The starting point for the resolution term is minimum bias data in which energy fluctuations are parameterized in terms of total energy in the event which itself is a function of the luminosity. This is weighted by S which is constrained from $|\vec{u}|$ distributions in the W data.

⁶⁾ α_{mb} must be adjusted for W data which have a different luminosity distribution.

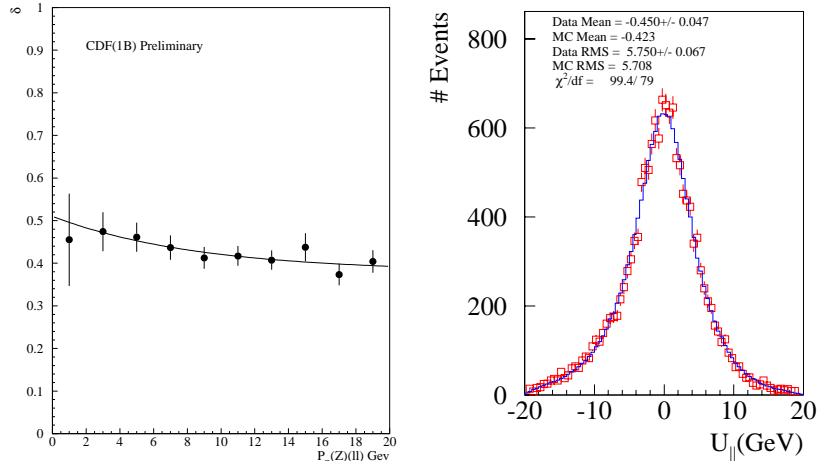


FIGURE 5. Left: Plot of $1 - R_{rec}$ vs. p_η for Z events. The points are both $Z \rightarrow ee$ and $Z \rightarrow \mu\mu$ events and the solid line is the fit to these points. Right: Comparison of u_\parallel from W data and simulation. The variable u_\parallel is the projection of \vec{u} onto the lepton momentum axis. This quantity should have a negative mean since the lepton is boosted in the direction of the W (opposite \vec{u}).

After obtaining the parameters for the recoil model, one can compare the simulation with W data. Figure 5 is one such comparison of u_\parallel in data and simulation from CDF. Comparisons from $D\bar{O}$ show similar agreement.

IV MONTE CARLO SIMULATION

The simulations used by both CDF and $D\bar{O}$ are similar in form. They start with a tree level calculation including parton distribution functions (PDF's). In an effort to separate out the various effects of the PDF's, $D\bar{O}$ parameterizes the Q^2 effect of the PDF's as $e^{-\beta Q}/Q$ where β is determined from Monte Carlo studies. The choice of which PDF to use is somewhat debatable. CDF attempts to constrain the allowed range of PDF's using W decay charge asymmetry data where the asymmetry is a function of the u to d ratio. The W lineshape is also dependent on this u-d ratio and thus the asymmetry can be used to set limits on the allowed PDF's. Unfortunately, the range of current PDF's does not fill the allowed asymmetry space making it difficult to use this method. $D\bar{O}$ has chosen a small set of recent PDF's and taken the variation as a systematic uncertainty.

NLO QCD contributions are incorporated using a calculation [3] which matches the $\mathcal{O}(\alpha_s^2)$ large q_T perturbative result with a small q_T soft gluon resummation. There are 3 parameters ($g1, g2, g3$) plus Λ_{QCD} in the most recent incarnation of this calculation. CDF fixes $g3$ to the Ladinsky-Yuan value and constrains $g1$ and $g2$ with Z data (Λ_{QCD} is varied by varying PDF's). $D\bar{O}$ sets $g1$ and $g3$ to the Ladinsky-Yuan values and constrains $g2$ with Z data while allowing Λ_{QCD} to vary within reasonable bounds.

The decay model includes QED radiative effects using a calculation by Berends

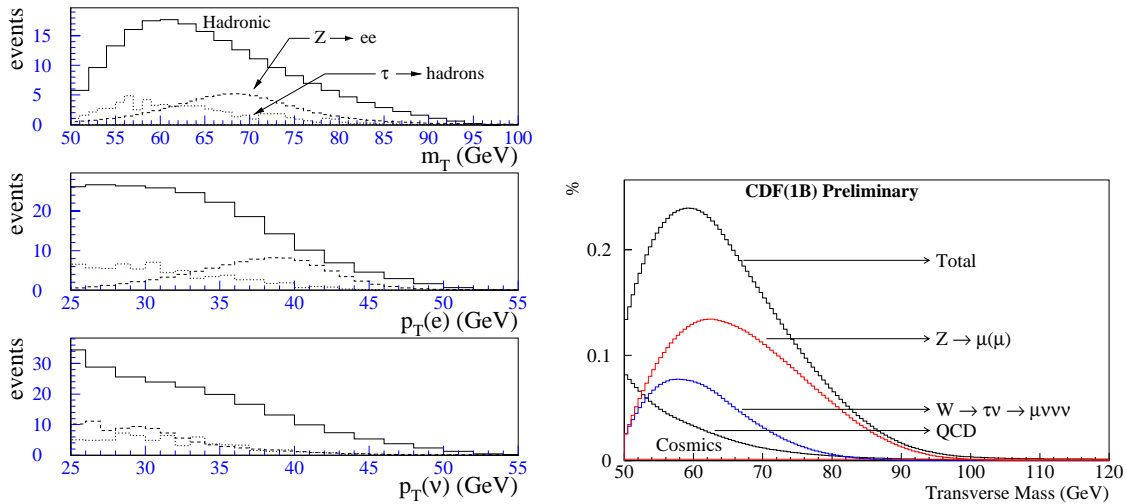


FIGURE 6. Left: $D\bar{0}$ background shapes for transverse mass and lepton and neutrino p_T distributions. The hadronic background is $(1.3 \pm 0.2)\%$, the Z background is $(0.42 \pm 0.08)\%$, and the $\tau \rightarrow \text{hadrons}$ is 0.24% . There is also a $W \rightarrow \tau\nu \rightarrow e\nu\nu\nu$ which is generated simultaneously with the $W \rightarrow e\nu$ events and contributes 1.6% events. Right: CDF background shapes for the transverse mass distribution. The dominant background is $Z \rightarrow \mu\mu$ where one muon is not detected in the tracking chamber and amounts to $(3.6 \pm 0.5)\%$. The other backgrounds are $W \rightarrow \tau\nu \rightarrow \mu\nu\nu$ at 0.8% , QCD at $(0.4 \pm 0.2)\%$, and Cosmic Rays which add $(0.1 \pm 0.05)\%$.

and Kleiss [4]. The results were checked by both CDF and $D\bar{0}$ using two-photon generators [5].

Backgrounds are included in the simulated lineshape and are detailed in Figure 6.

V RESULTS

The mass of the W is extracted using a likelihood fit of the Monte Carlo lineshapes to the data. The most precise value is obtained from fits to the transverse mass (Fig. 7).

The results for CDF and $D\bar{0}$ are

$$M_W^{D\bar{0}} = 80.44 \pm 0.12 \text{ GeV} \quad (7)$$

$$M_W^{CDF} = 80.43 \pm 0.16 \text{ GeV}. \quad (8)$$

The uncertainties in these measurements are documented in Table 1. Combining these numbers with previous measurements by CDF and $D\bar{0}$ and with measurements made by the LEP II experiments and NuTeV leads to a world average of

$$M_W = 80.420 \pm 0.055 \text{ GeV}. \quad (9)$$

These measurements are listed in Figure 8 together with the current best indirect

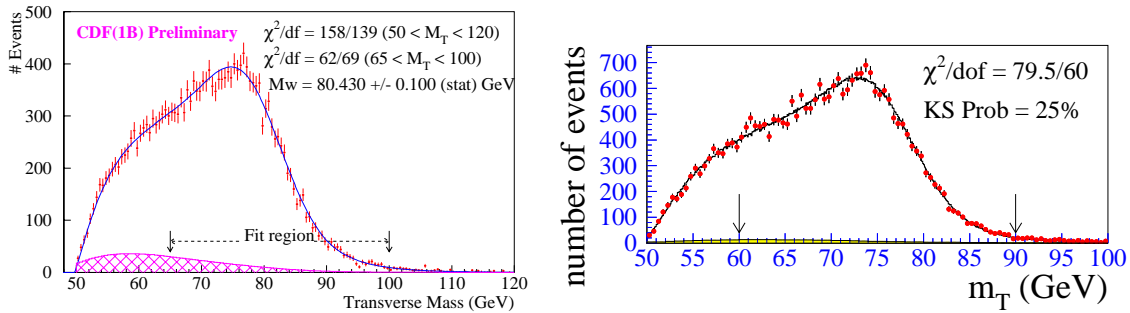


FIGURE 7. Left: CDF transverse mass distribution compared with simulation. The fit region is 65 to 100 GeV. Right: Same plot for DØ with a fit region of 60 to 90 GeV.

Uncertainty	CDF	DØ	
	(MeV)		
Statistical	100	70	} 95(stat)
Momentum / Energy Scale	40	65	
Calorimeter Linearity	–	20	
Lepton Resolution	25	20	
Recoil Modeling	90	40	
Input W p_T and PDF's	50	25	
Radiative Decays	20	15	
Higher Order Corrections	20	–	
Backgrounds	25	10	
Lepton Angle Calibration	–	30	
Fitting	10	–	
Miscellaneous	20	15	
Systematics Total	115	70	
Total (MeV)	155	120	

TABLE 1. Uncertainties in the W mass measurement for both CDF and DØ. It is suspected that the 90 MeV recoil modeling uncertainty for CDF is due in part to deficiencies in the model and should decrease in the final analysis. The energy scale uncertainty for DØ is dominated by the statistics of the Z data.

determination of M_W . Also in Figure 8 is a graphical representation of the state of the art in precision electroweak testing. The data point is the world average from above.

A The Future

CDF is currently working on adding the electron decay channel to the mass measurement while improving the muon result. The expectations are that the CDF uncertainty can be reduced to a little under 100 MeV. DØ is working on increasing the pseudorapidity range of accepted electrons by including those that

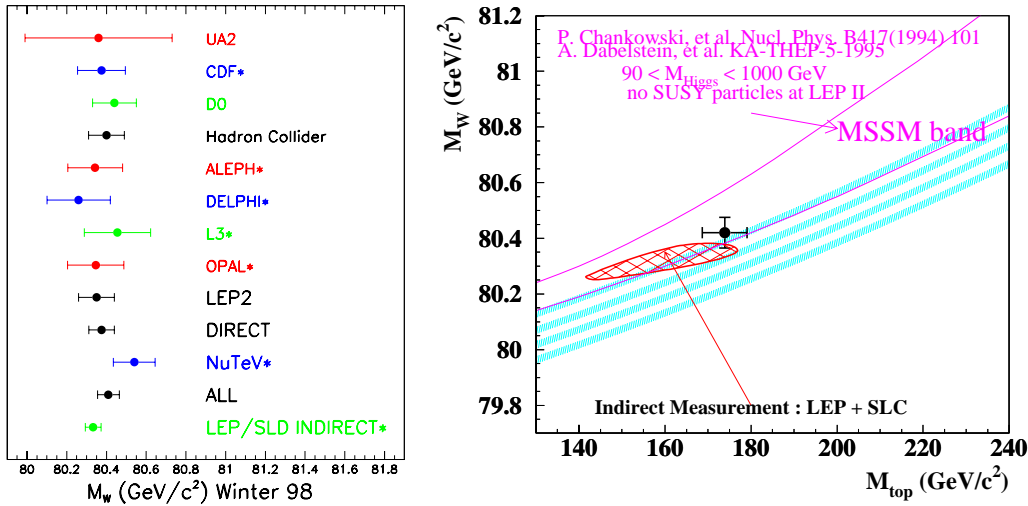


FIGURE 8. Left: W mass measurements from around the world. The CDF and DØ points are combined numbers from all their respective data taking runs. Right: W mass versus top mass for various higgs masses and SUSY.

traverse the endcap calorimeter. Here too, the aim is to reach 100 MeV.

Both experiments are also upgrading the detectors in preparation for Run 2 of the Tevatron which will bring a factor of 20 more data. With this larger dataset and a lot of perseverance on the part of the experimenters, the uncertainty is expected to reach ~ 40 MeV. Even farther in the future, TeV33 is supposed to supply another factor of 10 in data and a corresponding decrease in the W mass uncertainty, perhaps as low as 20-30 MeV.

REFERENCES

1. B. Abbott *et al.*, (DØ Collaboration), Phys. Rev. Lett. **80**, 3008 (1998), and submitted to Phys. Rev. D. More information on both the CDF and DØ measurements can be found at <http://www-cdf.fnal.gov/physics/ewk/ewk.html> and http://www-d0.fnal.gov/public/wz/ewk_public.html.
2. W. Hollik and W. Marciano, *Precision Tests of the Standard Electroweak Model*, ed. by P. Langacker (World Scientific, Singapore, 1994).
3. G.A. Ladinsky and C.P. Yuan, Phys. Rev. D **50**, 4239 (1994); P.B. Arnold and R.P. Kauffman, Nucl. Phys. B **349**, 381 (1991).
4. F.A. Berends and R. Kleiss, Z. Phys. C **27**, 365 (1985); F.A. Berends *et al.*, Z. Phys. C **27**, 155 (1985).
5. CDF used PHOTOS and DØ used a calculation by U. Baur *et al.*, Phys. Rev. D **56**, 140 (1997).